Article:
Fielding, L.A. and Armes, S.P. (2012) Preparation of Pickering emulsions and colloidosomes using either a glycerol-functionalised silica sol or core-shell polymer/silica nanocomposite particles. Journal of Materials Chemistry, 22 (22). 11235 - 11244. ISSN 0959-9428

https://doi.org/10.1039/c2jm31433a

Preparation of Pickering emulsions and colloidosomes using either a glycerol-functionalised silica sol or core-shell polymer/silica nanocomposite particles

Lee A. Fielding*[a] and Steven P. Armes[a]

Abstract. A commercial glycerol-modified 19 nm silica sol has been homogenised with sunflower oil to form stable Pickering emulsions and also covalently cross-linked colloidosomes. Colloidal core-shell polymer/silica nanocomposite particles produced using this glycerol-functionalised silica were also used to produce both Pickering emulsions and colloidosomes containing hybrid shells comprising both inorganic and organic components. The formation of stable oil-in-water Pickering emulsions required either low pH or the addition of electrolyte: this is rationalised in terms of the highly anionic surface character of the silica particles. Colloidosomes are readily obtained on addition of a polymeric diisocyanate, which reacts with the surface glycerol groups on the silica particles. This oil-soluble cross-linker is confined to the interior of the emulsion droplets, thus avoiding inter-colloidosome aggregation. The oil phase can be removed from the colloidosomes by washing with excess alcohol, resulting in microcapsules comprising either a 19 nm particulate silica shell or a 240 nm polymer/silica shell. These microcapsules can be imaged by optical microscopy in solution and by scanning electron microscopy in the dry state. The permeability of these colloidosomes with respect to small molecule release was also examined by incorporating an oil-soluble fluorescent dye during homogenisation that becomes water-soluble on raising the solution pH of the aqueous continuous phase. Finally, control experiments performed with a non-functionalised silica sol confirmed that Pickering emulsions cannot be converted into colloidosomes due to the absence of surface glycerol groups.

Introduction

Microcapsules with shells constructed from colloidal particles (colloidosomes[1]) have seen a surge of academic interest over the last decade,[2, 3] with capsules comprising polymer latex,[1, 4-14] inorganic sols,[15-18] nanocomposite particles[19] and quantum dots[20] being prepared. Colloidosomes are generally formed by the self-assembly of colloidal particles at an oil-water interface to form Pickering emulsions[21] followed by locking in the super-structure via annealing at elevated temperature,[1, 8, 14] gelling the internal phase[13, 16, 22] or inter-particle cross-linking.[6, 7, 14, 23, 24] We recently reported the fabrication of colloidosomes via covalent cross-linking of sterically stabilised latex particles at the oil-water interface.[5, 6] It was shown that an oil-soluble polymeric diisocyanate could cross-link latex-stabilised Pickering emulsion droplets from within the oil phase by reacting with hydroxy-functional steric stabiliser chains. Unfortunately, these capsules failed to significantly retard the release of an encapsulated small molecule dye over short time scales, with full release occurring within 20 h due to the highly permeable nature of the particulate shells. The formation of Pickering emulsions using colloidal particles such as silica sols[25, 26] and nanocomposite particles[27, 28] is well documented.[29] However, as far as we are aware, there is little literature precedent for the formation of stable colloidosomes using solely nano-sized silica or polymer/silica nanocomposite particles using cross-linking chemistry.

The preparation of colloidal nanocomposites comprising either conducting polymer-silica[30-34] or vinyl polymer-silica[35-42] has been widely reported.[43-45] It has been shown that such colloidal nanocomposites can act as pH-responsive Pickering emulsifiers,[27, 28] synthetic mimics for micrometeorites[46, 47] and high performance exterior architectural coatings.[48] Formulations for vinyl (co)polymer/silica nanocomposites are generally the most efficient (i.e. relatively high monomer conversions and silica aggregation efficiencies can be achieved) and often have a polymer core-silica shell morphology.[38, 39, 41] For example, Armes *et. al.* reported a highly efficient surfactant-free formulation for the preparation of colloidal polystyrene/silica,[40, 42] poly(methyl methacrylate)/silica[41] and poly(styrene-co-*n*-butyl acrylate)/silica[49] nanocomposite particles with well-defined core-shell particle morphologies and up to 95 % silica aggregation efficiency. In this formulation, the key to success is the use of a commercially available glycerol-functionalised aqueous silica sol (Bindzil CC40)[50] in combination with a cationic azo initiator.

Herein we describe the formation of Pickering emulsions using commercially available unmodified and glycerol-functionalised aqueous silica sols. Furthermore, core-shell polymer/silica nanocomposite particles prepared using the glycerol-functionalised silica sol are also used to successfully stabilise Pickering emulsions. The conditions required for successful emulsification are investigated and the resulting Pickering emulsions are characterised in terms of their emulsion type and droplet size distributions. The glycerol functionality on the silica particle surface is then utilised to covalently cross-link the Pickering emulsions using an oil-soluble polymeric diisocyanate in order to form stable colloidosomes comprising either 19 nm silica or 240 nm polymer/silica nanocomposite shells (see Figure 1). These colloidosomes are studied by optical and electron microscopy and the release of a pH-responsive dye from their interior is investigated.

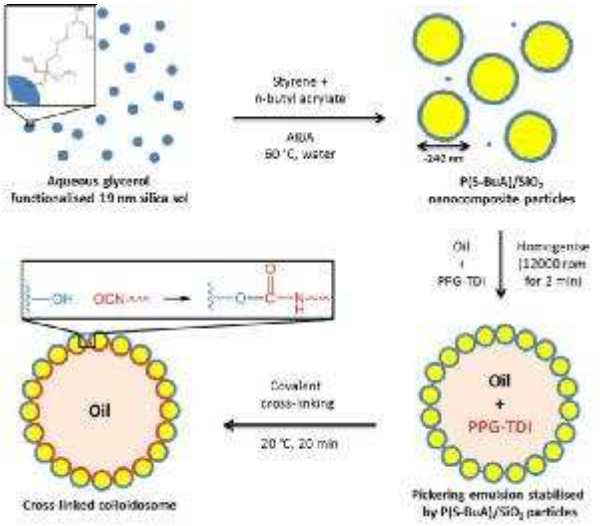

Fig. 1 Preparation of poly(styrene-co-*n*-butyl acrylate)/silica nanocomposite particles by aqueous emulsion polymerisation at 60 °C, followed by addition of oil and homogenisation to form a Pickering emulsion. The nanocomposite particles stabilising the emulsion droplets can be covalently-stabilised using an oil-soluble PPG-TDI cross-linker to form stable colloidosomes.

Experimental Section

Materials

Styrene (S) and *n*-butyl acrylate (BuA) were purchased from Aldrich, passed in turn through a basic alumina column to remove inhibitor and stored at -20 °C prior to use. 2,2'-Azobis(isobutyramidine) dihydrochloride (AIBA), *n*-dodecane, sunflower oil, fluorescein and tolylene 2,4-diisocyanate-terminated poly(propylene glycol) [PPG-TDI] were purchased from Aldrich and used as received. Ethanol and iso-propanol were purchased from Fisher and used as received. Glycerol-functionalised silica sol (Bindzil CC40; 37 wt. % aqueous dispersion; TEM number-average diameter = 19 nm) and unmodified silica (Bindzil 2040, 40 wt. % aqueous dispersion, TEM number-average diameter = 20 nm) were supplied by Eka Chemicals (Bohus, Sweden), which is a division of AkzoNobel (Netherlands). Deionised water obtained from an Elgastat Option 3A water purifier was used in all experiments.

Nanocomposite Synthesis

For the poly(styrene-co-*n*-butyl acrylate)/silica particles, Bindzil CC40 silica sol (95 g) was added to deionised water (352 ml) and the solution was degassed using nitrogen. Styrene (25 g) and n-butyl acrylate (25 g) monomer were then added and the solution was heated to 60 °C with magnetic stirring at 250 rpm. The polymerisation was initiated by the addition of AIBA (500 mg) dissolved in degassed, deionised water (5.0 ml) and allowed to proceed for 24 h. A further charge of AIBA initiator (100 mg) was added after this time in order to oligomerise unreacted monomer present. Any excess silica was removed by centrifugation at 5 °C using a refrigerated centrifuge, followed by redispersion of the sedimented nanocomposite particles in water. The polystyrene/silica particles were prepared using an almost identical protocol using 57 g Bindzil CC40 silica, 51 g styrene monomer, 500 mg AIBA and 396 g water.

Preparation of Pickering Emulsions and Colloidosomes

PPG-TDI (0 - 79 mg) was weighed into a sample vial and then dissolved in either sunflower oil or n-dodecane (5.0 ml). This solution was homogenised for 2 minutes with 5.0 ml of an aqueous solution at pH 3 - 10 containing 0.1 - 5.0 wt. % of either nanocomposite particles or silica sol using a IKA Ultra-Turrax T-18 homogeniser equipped with a 10 mm dispersing tool and operating at 12,000 rpm. The resulting emulsions were allowed to stand at room temperature for at least 60 minutes to allow the urethane cross-linking reaction to occur.

Encapsulation and Release Studies

Fluorescein (1 mg) and PPG-TDI (40 mg) were added in turn to a sample vial and dissolved in sunflower oil (5.0 ml). This mixture was homogenised for 2 minutes with 5.0 ml of an aqueous acidic solution (pH 3.0) containing 0.1 – 5.0 wt. % of either polymer/silica nanocomposite particles or silica sol using a IKA Ultra-Turrax T-18 homogeniser equipped with a 10 mm dispersing tool and operating at 12,000 rpm. The resulting emulsions were allowed to stand at room temperature for at least 60 minutes to allow the urethane cross-linking reaction to occur. Release studies were conducted using a Perkin-Elmer Lambda 25 UV/visible spectrophotometer operating in time drive mode. A known volume (20 µl) of colloidosomes was placed on top of an aqueous solution (3.0 mL, pH 9) in a plastic cuvette equipped with a magnetic stirrer. The absorbance at 490 nm due to the released dye was monitored as a function of time. Since the colloidosomes are less dense than water, they remain at the top of the cuvette and hence do not pass in front of the transmitted beam. As a control experiment, pure oil containing the same concentration of dissolved dye was used instead of colloidosomes.

Dynamic light scattering (DLS)

Studies were conducted at 25 °C using a Malvern Zetasizer Nano ZS instrument equipped with a 4 mW He-Ne solid-state laser operating at 633 nm. Back-scattered light was detected at 173° and the mean particle diameter was calculated over thirty runs of ten seconds duration from the quadratic fitting of the correlation function using the Stokes-Einstein equation. All measurements were performed in triplicate on highly dilute aqueous dispersions.

Laser diffraction

A Malvern Mastersizer 2000 instrument equipped with a small volume Hydro 2000SM sample dispersion unit (ca. 50 mL), a He-Ne laser operating at 633 nm, and a solid-state blue laser operating at 466 nm was used to size the emulsions. The stirring rate was adjusted to 1,000 rpm in order to avoid creaming of the emulsion during analysis. Corrections were made for background electrical noise and laser scattering due to contaminants on the optics and within the sample. After each measurement, the cell was rinsed three times with isopropanol, followed by three washes with distilled water. The cell walls were wiped with lens cleaning tissue to avoid cross-contamination and the laser was aligned centrally on the detector. In general, the emulsions were analysed five times and the data were averaged. The raw data were analysed using Malvern software and the mean droplet

Table 1 Surface functionality, surface area, density and measured mean particle diameters of the two colloidal silica sols used in this work.

Entry no.	Silica surface functionality	BET surface area (A_s) / $m^2 g^{-1}$	Density (ρ) [a] / g cm^{-3}	BET diameter (d) [b] / nm	Number-average diameter [c] / nm	Weight-average diameter [d] / nm	Intensity-average diameter [e] / nm
1	Glycerol	157	2.04	19	19	22	21
2	None (Silanol)	118	2.19	23	20	23	27

[a] Determined by helium pycnometry. [b] Determined using $d = 6 / A_s.\rho$ assuming a spherical morphology and non-porous particles [c] Determined using TEM by counting at least 100 particles. [d] Determined using small angle x-ray scattering.[51, 52] [e] Determined by dynamic light scattering; the polydispersity index is given in brackets.

diameter was taken to be the volume-average diameter ($D_{4/3}$) which is mathematically expressed as $D_{4/3} = \Sigma D_i^4 N_i / \Sigma D_i^3 N_i$.

Disc centrifuge photosedimentometry (DCP)

A CPS Instruments model DC24000 instrument was used to obtain weight-average particle size distributions of the nanocomposite particles. The disc centrifuge was operated at 16 000 rpm and the spin fluid contained a density gradient constructed from 12.0 to 4.0 wt. % aqueous sucrose solutions; a small volume of *n*-dodecane (0.50 ml) was used to inhibit surface evaporation in order to extend the lifetime of the gradient. The disc centrifuge was calibrated with a poly(vinyl chloride) latex with a weight-average particle diameter of 263 nm. For each sample, the mean dry particle density as measured by helium pycnometry was used to calculate the weight-average particle diameters. It has been recently shown that the weight-average diameter reported by DCP for core-shell polystyrene/silica nanocomposite particles is subject to a sizing artefact due to their inherent density distribution, which in principle can be reanalysed and corrected.[53] However, no such correction was applied in the present work. Hence the DCP standard deviation should be treated as an underestimate of the true width of the particle size distribution.

Optical Microscopy

Optical microscopy images were recorded with a Motic BA300 light microscope fitted with a digital camera.

Helium pycnometry

The solid-state densities of the dried polymer/silica nanocomposite particles and silica sols were measured using a Micrometritics AccuPyc 1330 helium pycnometer at 20 °C.

Thermogravimetric analysis (TGA)

Analyses were conducted on freeze-dried particles, which were heated in air to 800 °C at a heating rate of 20 °C min^{-1} using a TA Instruments Q500 thermogravimetric analyser. The observed mass loss was attributed to complete pyrolysis of the copolymer component, with the remaining incombustible residues being attributed to pure silica (SiO_2).

Transmission electron microscopy (TEM)

Images were recorded using a Phillips CM100 microscope operating at 100 kV by drying a drop of dilute aqueous nanocomposite or silica sol dispersion onto a carbon-coated copper grid.

Field emission scanning electron microscopy (FE-SEM)

Images were recorded using a FEI Inspect instrument operating at 20 to 30 kV for samples dried onto carbon discs and sputter-coated with gold. Colloidosome samples were washed repeatedly with isopropanol to remove any traces of oil and dried directly onto aluminum stubs before sputter-coating.

Aqueous electrophoresis

Zeta potentials were calculated from electrophoretic mobilities using a Malvern Zetasizer NanoZS instrument equipped with an autotitrator (Malvern MPT-1) in the presence of 1.0 mM KCl as a background salt. The solution pH was initially adjusted to pH 11 by the addition of KOH and subsequently titrated to pH 1.5 using HCl; zeta potential measurements were conducted as a function of pH.

Results and Discussion

Characterisation of silica sols and nanocomposite particles

Commercial silica sols are readily available over a wide range of sizes, media and surface functionalities. In this study, two nano-sized aqueous silica sols are used to prepare Pickering emulsions; the surface area, density and particle diameters of these sols are summarised in Table 1. Glycerol-functionalised Bindzil CC40 silica sol (entry 1, Table 1) is a commercially available product based on surface derivatisation of a conventional anionic silica sol. In order to produce the glycerol functionality, the precursor silica sol is reacted with (3-glycidyloxypropyl)trimethoxysilane. The commercial glycerol-functionalised silica sol used in the present study typically has one to two glycerol groups per nm^2.[50, 54] The surface area and density of the dried particles are 157 $m^2 g^{-1}$ and 2.04 g cm^{-3} respectively, resulting in a calculated mean particle diameter of 19 nm. As expected, the mean diameters obtained from TEM, SAXS and DLS all correlate well with this BET value (see Table 1). Bindzil 2040 (entry 2, Table 1) is a conventional aqueous anionic silica sol with a surface area of 118 $m^2 g^{-1}$, a density of 2.19 g cm^{-3} and measured mean particle diameter of 20-27 nm. In this study it is used to prepare Pickering emulsions and also as a control in the preparation of covalently cross-linked colloidosomes. Representative TEM images of these two silica sols are shown in Figures 2A and 2B.

Colloidal polystyrene/silica and poly(styrene-co-*n*-butyl acrylate)/silica nanocomposite particles were prepared by aqueous emulsion polymerisation using scaled-up protocols of those reported by Schmid *et al.*[42, 49] Table 2 summarises the nanocomposite particles investigated in this work. Entry 1 is a poly(styrene-co-*n*-butyl acrylate)/silica nanocomposite prepared using a 50:50 comonomer ratio, with an apparent weight-average diameter of 207 ± 70 nm and a mean silica content of 39 wt. %. Entry 2 is a polystyrene/silica nanocomposite with a weight-average diameter of 321 ± 60 nm and a mean silica content of 23 wt. %. The scale of the polymerisation (50 g versus 5 g monomer) does not appear to affect the particles; their mean

Table 2 Summary of the two polymer/silica nanocomposites used in this work. Both samples were prepared by aqueous emulsion polymerisation at 60 °C using a commercial 19 nm silica sol (Bindzil CC40) and cationic AIBA initiator.[a]

Entry no.	St : BuA comonomer ratio	Weight-average diameter [b] / nm	Intensity-average diameter [c] / nm	Silica content [d] / wt. %	Density [e] / g cm^{-3}
1	50 : 50	207 ± 70	226 (0.069)	39	1.37
2	100 : 0	321 ± 60	422 (0.070)	23	1.24

[a] Polymerisations were conducted using 50 g total comonomer in a total reaction mass of 500 g at 60 °C for 24 h; in both cases the final monomer conversion was greater than 90 %. [b] As determined by disc centrifuge photosedimentometry. [c] As determined by dynamic light scattering, the polydispersity index is given in brackets. [d] Determined by thermogravimetric analysis. [e] Determined by helium pycnometry.

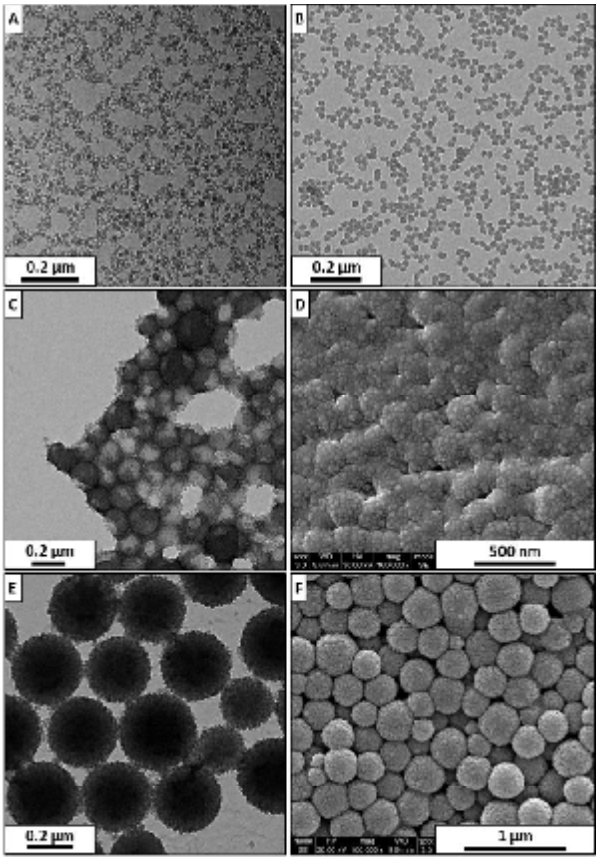

Fig. 2 Representative TEM and SEM images of (A) glycerol-functionalised 19 nm silica, (B) 20 nm non-functionalised silica sol, (C+D) poly(styrene-co-*n*-butyl acrylate)/silica nanocomposites and (E+F) polystyrene/silica nanocomposite particles.

diameter, density and silica content correlate well with values previously reported by Schmid et al.[42, 49] It is already known thatsuch nanocomposite particles have a well-defined 'core-shell' morphology with a polymeric core and a particulate silica shell.[42, 49, 51] Furthermore, the use of glycerol-functionalised 19 nm silica particles (in comparison with non-functionalised silica) is essential for successful nanocomposite formation[42] and the interaction between the surface glycerol groups on the silica particles with the polymeric core has been investigated by solid-state NMR studies.[55]

Figure 2 shows TEM and SEM images of the glycerol-functionalised 19 nm colloidal silica and the 20 nm non-functionalised silica sol (images A + B), poly(styrene-co-*n*-butyl acrylate)/silica (images C + D) and polystyrene/silica nanocomposite particles (images E + F) used in this work. Both of these colloidal nanocomposites clearly have silica-rich surfaces, as previously confirmed by several techniques including aqueous electrophoresis,[42, 49] x-ray photoelectron spectroscopy[42, 49] and small-angle x-ray scattering.[51] Furthermore, it is apparent that the poly(styrene-co-*n*-butyl acrylate)/silica particles begin to coalesce on the SEM stub due to their sub-ambient T_g; upon drying, these nanocomposites form transparent free-standing films.[49] As expected, the high T_g polystyrene/silica nanocomposite particles do not coalesce and remain as discrete spherical particles.

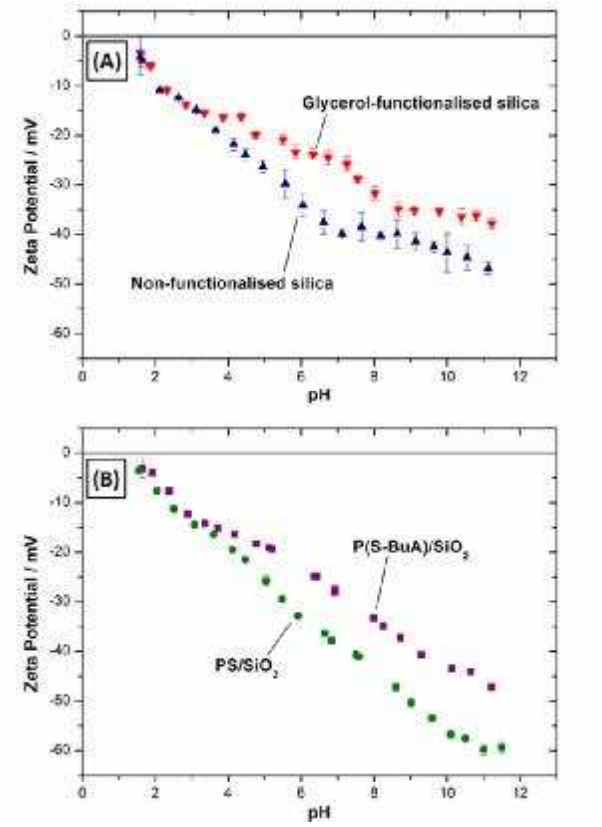

Fig. 3 Aqueous electrophoresis curves obtained for (A) glycerol-functionalised and non-functionalised silica sols (entries 1 and 2, Table 1); (B) 50:50 poly(styrene-co-*n*-butyl acrylate)/silica and polystyrene/silica nanocomposite particles (entries 1 and 2, Table 2).

Pickering emulsions

The conditions required to form stable Pickering emulsions using 12 nm colloidal silica particles with toluene as the oil phase have previously been investigated by Binks and Lumsdon.[26] It was

shown that the stability of Pickering emulsions towards both creaming and coalescence depends on the solution pH, electrolyte concentration and type of electrolyte used. In the presence of NaCl, it was found that the Pickering emulsions had a maximum stability towards coalescence at pH 4, which corresponds to a relatively low negative zeta potential for the silica particles. At high pH, the silica particles became too anionic to act as effective Pickering emulsifiers. Similar observations were made by Blute *et al*. for the preparation of foams stabilised by colloidal silica sols.[56] In general, the foamability of these sols was found to be greatest when the silica had the lowest degree of hydrophilicity (i.e. at low pH) and at higher particle concentrations.

Although the glycerol-modified silica sol is likely to behave in a similar manner to non-functionalised silica particles, there is no doubt that the surface modification reduces their anionic charge compared to untreated silica sols (Figure 3A). In order to investigate the conditions required for successful emulsion formation, 5.0 ml of a 5.0 wt. % aqueous silica sol was homogenised with 5.0 ml sunflower oil for 2 minutes at 12,000 rpm. Both non-functionalised and glycerol-functionalised silica were investigated and the solution pH was varied from pH 2 to10.

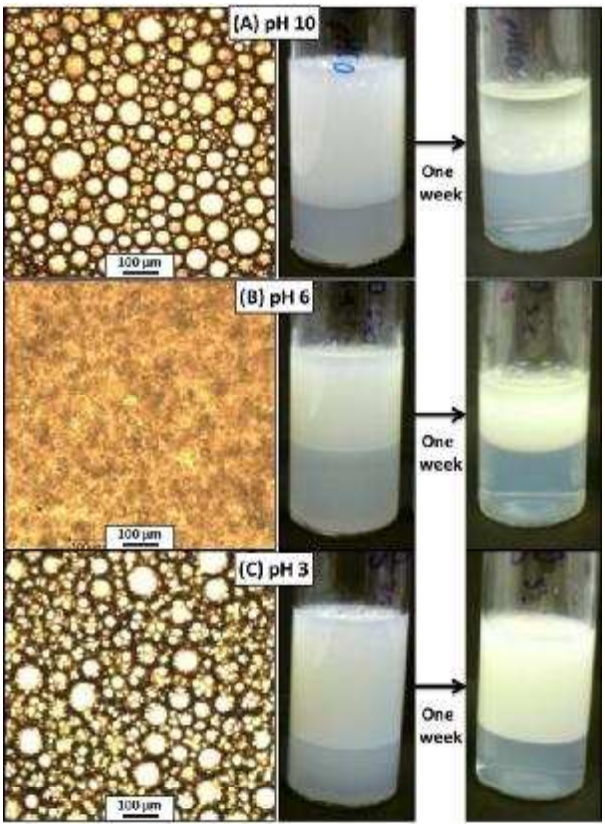

Fig. 4 Optical micrographs and digital photographs of Pickering emulsions prepared by homogenising 5.0 ml sunflower oil and 5.0 ml of 5.0 wt. % aqueous Bindzil 2040 silica sol at (A) pH 10, (B) pH 6 and (C) pH 3. The mixtures were homogenised for 2 minutes at 12,000 rpm and allowed to stand for 1 h before optical micrographs and digital photographs were recorded. After one week, the Pickering emulsions were re-analysed: it was found that both (A) and (B) had demulsified, whereas (C) remained stable.

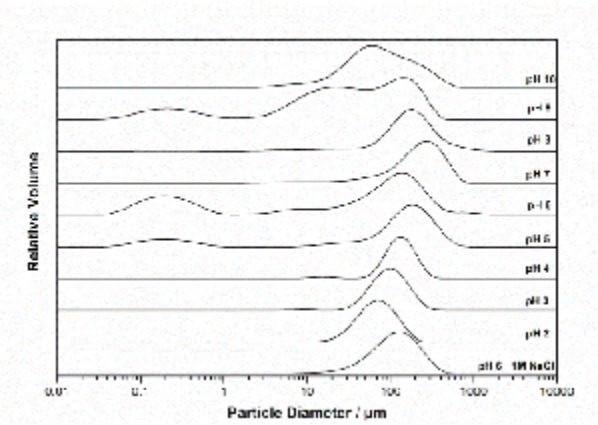

Fig. 5 Droplet size distributions obtained using laser diffraction for Pickering emulsions prepared using 5.0 ml sunflower oil and 5.0 ml of 2.7 wt. % aqueous poly(styrene-co-*n*-butyl acrylate)/silica particles. Particle size distributions were recorded for emulsions prepared with solution pH between 10 and 6. The addition of 1 M NaCl electrolyte at pH 6 enhanced emulsion stability compared to emulsions prepared in the absence of added salt.

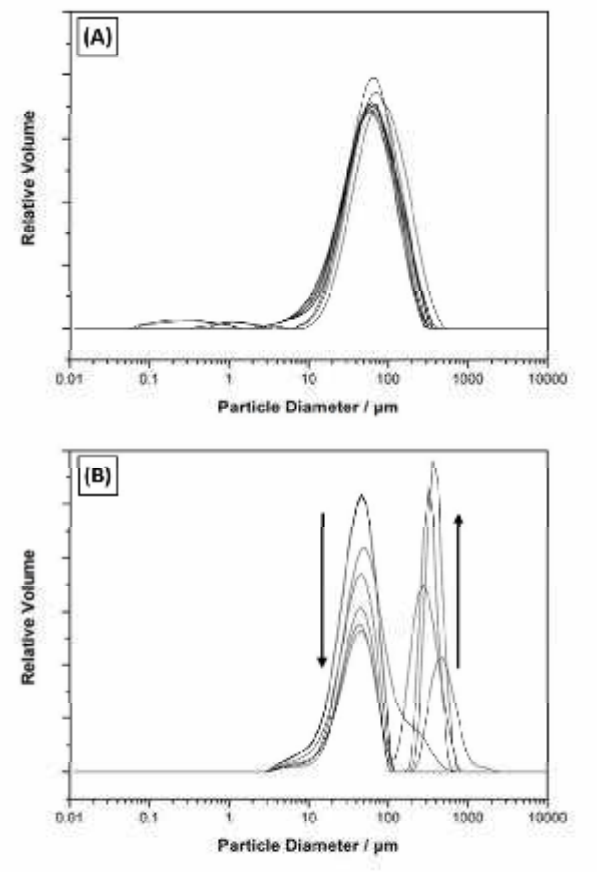

Fig. 6 Droplet size distributions obtained using laser diffraction when emulsion droplets are transferred to an alkaline solution (pH 10) for: (A) covalently cross-linked colloidosomes prepared using 5.0 ml sunflower oil, 49 mg PPG-TDI and 5.0 ml of 2.5 wt. % aqueous poly(styrene-co-*n*-butyl acrylate)/silica particles at pH 3; (B) Pickering emulsion droplets prepared using 5.0 ml sunflower oil and 5.0 ml of 2.5 wt. % aqueous poly(styrene-co-*n*-butyl acrylate)/silica particles at pH 3.

The resulting mixtures were analysed via optical microscopy and laser diffraction in order to assess successful Pickering emulsion formation. Figure 4 shows optical micrographs and digital photographs of emulsions prepared using unmodified silica at pH 10, 6 and 3. As expected, no emulsion is formed at pH 6 and the two liquids phase-separate rapidly. At pH 10 and 3, Pickering emulsions can be observed both visually and by optical microscopy. However, within one week the emulsion prepared at pH 10 demulsified to form two separate phases whereas the corresponding emulsion stabilised using silica at pH 3 remained stable for at least this time period. The formation of a stable Pickering emulsion was expected at low pH due to the relatively low surface charge of the silica particles, as previously reported by Binks and Lumsdon[26] for Pickering emulsions and Blute *et al.*[56] for foams. The observations made for the glycerol-functionalised silica were almost identical to those for the unmodified particles.

Figure 5 shows the typical droplet size distributions obtained when aqueous poly(styrene-co-*n*-butyl acrylate)/silica particles (entry 1, Table 2) were homogenised with sunflower oil. It is perhaps worth noting that the majority of the Pickering emulsions

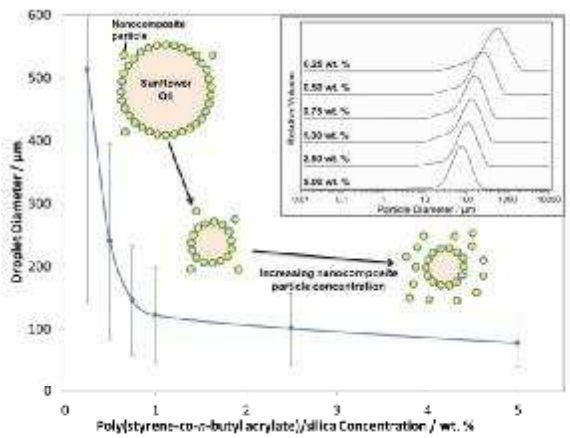

Fig. 7 Volume-average droplet diameter vs. nanocomposite particle concentration for Pickering emulsions prepared using 5.0 ml sunflower oil and 5.0 ml of aqueous poly(styrene-co-*n*-butyl acrylate)/silica particles at pH 3. The inset shows the particle size distributions recorded for each measurement. The mixtures were homogenised for 2 minutes at 12,000 rpm and allowed to stand for 1 h before their particle size distributions were recorded using laser diffraction.

prepared in this work have relatively broad droplet size distributions. Established methods such as membrane emulsification[57, 58] or the use of a microfluidic device[24] could possibly yield more monodisperse emulsions, but these techniques are beyond the scope of this work. Stable Pickering emulsions were obtained using aqueous nanocomposite particles at low pH. The smallest, most stable oil droplets were obtained at pH 2 when the silica particles and hence nanocomposite particles have their lowest surface charge (Figure 3). At both pH 3 and 4, stable emulsions were obtained with mean droplet diameters of approximately 100 μm. Above this pH unstable emulsions were obtained, as evidenced by the multi-modal droplet size distributions and increase in the signal due to free nanocomposite particles at around 200 nm. Furthermore, both nanocomposite and silica-stabilsed Pickering emulsions prepared at low pH are pH-sensitive; i.e. demulsification can be triggered by the addition of base to these emulsions, as confirmed by laser diffraction (see Figure 6B). This inherent instability at higher pH can be counteracted by the addition of electrolyte. For example, stable Pickering emulsions can be prepared at pH 6 when 1 M NaCl is used as a background salt (see Figure 5). In essence, the conditions for successful Pickering emulsion formation require either low pH and/or added salt to reduce or screen the silica surface charge. These conditions are required for both the anionic glycerol-functionalised 19 nm silica and the polymer/silica nanocomposite particles. This is unsurprising given the core-shell morphology of the nanocomposite particles, which ensures a silica-rich surface composition.

The concentration dependence of the sunflower oil droplet diameter was investigated by homogenising equal volumes of oil with aqueous dispersions containing various concentrations of particles at pH 3. Figure 7 shows the volume-average sunflower oil droplet diameter obtained for a series of poly(styrene-co-*n*-butyl acrylate)/silica dispersions at concentrations of 0.25 to 5.00 wt. %, the droplet size distributions in each case are displayed in the inset. At low particle concentrations (< 1.0 wt. %), large

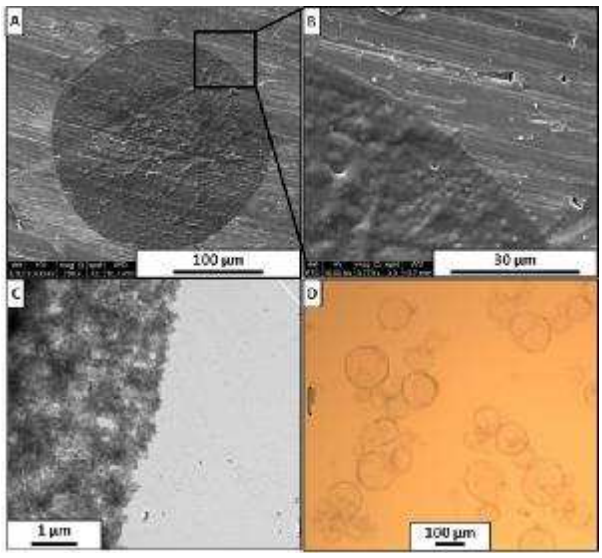

Fig. 8 Covalently cross-linked colloidosomes prepared using 5.0 ml sunflower oil, 45 mg PPG-TDI and 5.0 ml of 1.0 wt. % aqueous poly(styrene-co-*n*-butyl acrylate)/silica particles at pH 3. The mixtures were homogenised for 2 minutes at 12,000 rpm and allowed to stand for 1 h before washing with excess isopropanol. Image (A) shows an SEM image of a collapsed colloidosome and (B) its magnified leading edge; (C) is a TEM image of the leading edge of a single colloidosome, showing the 19 nm silica particles within the polymeric phase. An optical micrograph of the colloidosomes that survive after an alcohol challenge is shown in image (D).

relatively unstable emulsion droplets are formed with small quantities of excess nanocomposite particles present in the aqueous phase after creaming. The sunflower oil droplet size becomes approximately constant (100 – 120 μm) above particle concentrations of 1.0 wt. %, with the excess nanocomposite particles remaining in the lower aqueous phase (as indicated by a turbid rather than transparent solution). These observations are similar to those made for emulsions made with 107 nm poly(glycerol monomethacrylate)-stabilised polystyrene latex

particles prepared by Thompson *et al.*[6] However, in this case the latex was a rather more efficient Pickering emulsifier, since no excess latex was present at concentrations below 1.5 wt. %.

Colloidosomes

Stable Pickering emulsions can be easily prepared using 19 nm silica sol or polymer/silica nanocomposite particles at low pH and/or in the presence of added salt. Moreover, the glycerol functionality on the surfaces of these particles may be utilised to form covalently cross-linked colloidosomes, as previously demonstrated by Thompson *et al.* for glycerol-functionalised latexes.[5, 6] This can be achieved by dissolving an oil-soluble polymeric diisocyanate (PPG-TDI) in the sunflower oil phase prior to homogenisation with the aqueous phase. Emulsification allows the isocyanate groups to react with the surface glycerol groups on the silica particles to form urethane bonds. If these urethane linkages form cross-links between adjacent silica particles around the emulsion droplets, the superstructure can be locked into place forming colloidosome microcapsules.

The integrity of these colloidosomes can be readily tested using an 'alcohol challenge' whereby the oil droplet phase is completely removed using excess isopropanol.[5-7] Non-crosslinked Pickering emulsions stabilised with either colloidal silica or nanocomposite particles do not survive such a challenge. However, in the case of cross-linked colloidosomes, the internal oil phase is removed but the shell should remain intact. The resulting hollow shells can be observed by optical microscopy and SEM.

Figure 8D shows a typical optical micrograph obtained for a poly(styrene-co-*n*-butyl acrylate)/silica nanocomposite Pickering emulsion prepared using PPG-TDI after an alcohol challenge. The surviving colloidosome microcapsules provide good evidence for effective inter-particle cross-linking; when an alcohol challenge is conducted on non-cross-linked emulsions, no microcapsules are observed. SEM images of the dried colloidosomes are shown in Figures 8A and 8B. In all cases the colloidosomes are fully collapsed due to the ultra-high vacuum conditions and appear to be 2D 'pancakes', rather than hollow spheres. Unfortunately, the low T_g of these poly(styrene-co-*n*-butyl acrylate)/silica particles causes their coalescence upon drying to form a nanocomposite film; making it difficult to observe the individual particles by SEM. Figure 8C shows a TEM image of the edge of a single collapsed colloidosome, in this case the individual nanocomposite particles are better resolved with 19 nm silica particles discernible within the structure.

In order to better visualise the particulate shell of the colloidosomes, poly(styrene-co-*n*-butyl acrylate)/silica nanocomposites were replaced with the higher T_g polystyrene/silica particles (entry 2, Table 2). These particles stabilise sunflower oil-in-water emulsions under the same conditions as previously discussed and thus could be used to form cross-linked colloidosomes. Figure 9 shows images obtained for these polystyrene/silica colloidosomes after an alcohol challenge. The most noticeable difference is that there appears to be a large degree of debris in both the optical micrograph and the SEM images. This is most likely due to a combination of free (non-adsorbed) nanocomposite particles remaining after homogenisation (thus not cross-linked) and fragments of partially cross-linked nanocomposite colloidosomes which have detached from the microcapsules. Nevertheless, some intact colloidosomes are present in these micrographs and the individual

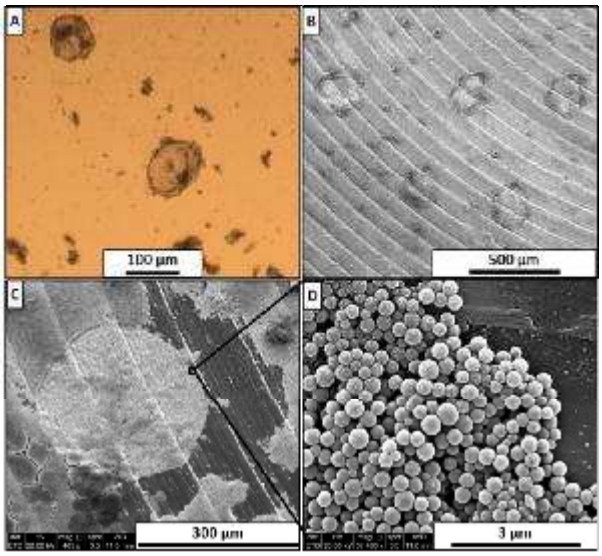

Fig. 9 Covalently cross-linked colloidosomes prepared using 5.0 ml sunflower oil, 45 mg PPG-TDI and 5.0 ml of 2.7 wt. % aqueous polystyrene/silica particles at pH 3. The mixtures were homogenised for 2 minutes at 12,000 rpm and allowed to stand for 1 h before washing the oil phase with excess isopropanol. (A) shows an optical micrograph of the colloidosomes that survive an alcohol challenge, (B, C and D) are SEM images at increasing magnification of collapsed colloidosomes, with image (D) showing the highly magnified leading edge of the colloidosome in (C), which confirms its particle microstructure.

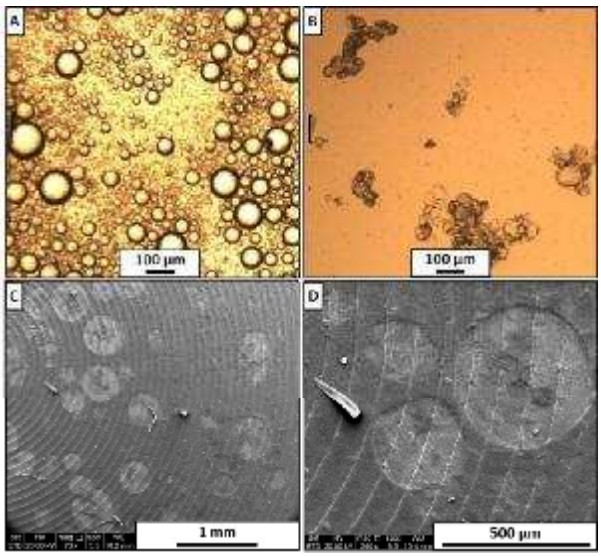

Fig. 10 Covalently cross-linked colloidosomes prepared using 5.0 ml sunflower oil, 45 mg PPG-TDI and 5.0 ml of 1.0 wt. % aqueous glycerol-functionalised silica particles at pH 3. The mixtures were homogenised for 2 minutes at 12,000 rpm and allowed to stand for 1 h before the optical micrograph in (A) was taken. Image (B) shows an optical micrograph recorded for the surviving colloidosomes after washing with excess isopropanol and (C + D) are SEM images of the dried colloidosomes, which collapse completely under ultra-high vacuum conditions.

nanocomposite particles can be observed by SEM and TEM. As expected, the colloidosome shells closely resemble the original particles shown in Figure 2F, i.e. they are spherical and clearly decorated with silica particles.

Since the surface glycerol groups on the silica nanoparticles in the shell of the nanocomposite particles can be reacted with PPG-TDI to form covalently cross-linked colloidosomes, it follows that microcapsules comprising ultrathin 19 nm silica shells can be formed. This is indeed the case; when PPG-TDI is present in the oil phase prior to homogenisation with aqueous Bindzil CC40, covalently cross-linked colloidosomes are observed. Figure 10A shows an optical micrograph of sunflower oil-in-water droplets stabilised by the glycerol-functionalised silica sol. When such colloidosomes are washed with isopropanol, intact microcapsules can be observed (Figure 10B). These silica colloidosomes are generally much harder to visualise using optical microscopy than those prepared using nanocomposite particles. This is due to their much thinner shells. As the isopropanol begins to evaporate from the microscope slide, the colloidosomes begin to aggregate and eventually collapse, allowing higher contrast images to be recorded.

Figures 10C and 10D show SEM images of collapsed silica colloidosomes, which appear as approximately circular imprints on the stub rather than protruding from its surface. This is a result of the large quantity of excess silica present in the sample (and thus on the stub). As the isopropanol solution is deposited onto the SEM stub, the colloidosomes will be large and spherical. Once the isopropanol evaporates the free silica will deposit around the edges of the colloidosomes forming a relatively thick silica layer. After collapsing, the remaining silica 'pancake' will be only two particles thick, thus appearing as an imprint on the stub. This is fortuitous: when silica colloidosomes are viewed by SEM with no excess silica present, no microcapsules can be detected due to the nano-sized dimensions of the silica sol.

A control experiment using unmodified silica (entry 2, Table 1) confirmed the importance of having glycerol functionality on the surface of the silica particles. As previously demonstrated, these unmodified silica particles readily stabilise Pickering emulsions at low pH. However, when PPG-TDI is incorporated into the oil phase and the resulting emulsion is challenged with isopropanol, no intact colloidosomes are observed either by SEM or optical microscopy. This negative control experiment highlights the requirement for surface glycerol groups to form covalently cross-linked colloidosomes.

Pickering emulsions prepared either with silica or nanocomposite particles are sensitive to the addition of base, whereas covalently cross-linked colloidosomes are insensitive. This is demonstrated in Figure 6, whereby covalently cross-linked colloidosomes prepared using poly(styrene-co-*n*-butyl acrylate)/silica nanocomposite particles at pH 3 retain their droplet size distribution when transferred to water at pH 10. In contrast, when the analogous non-cross-linked Pickering emulsion is transferred to water at pH 10, substantial demulsification is observed within 5 minutes. This differing stability supports the successful formation of covalently cross-linked microcapsules under the former conditions.

Release of small molecules from colloidosomes

It has previously been shown that small molecule fluorescent dyes are rapidly released from colloidosomes prepared from sterically stabilised latexes.[6] Microcapsule permeability could be reduced by the deposition of a polypyrrole overlayer, although not significantly. Furthermore, it was suggested that the size of the intrinsic packing defects present in the colloidosome shell is directly related to the size of the species that can be retained. The approximate packing defect dimensions were suggested to be 0.7 times the size of the latex particles comprising the colloidosome shell. Recently, Williams et al.[59] demonstrated that the release of a small molecule dye from colloidosomes comprising disordered nano-sized Laponite clay platelets also occurs within a short time scale (15 h), suggesting that the encapsulation of a molecular species (e.g. a dye) is highly problematic.

In order to compare the encapsulation behaviour of the nanocomposite colloidosomes with previous studies, the release of fluorescein dye was investigated. Fluorescein is an oil-soluble compound with a pK_a of 6.3 and hence remains water-insoluble at low pH. When exposed to alkaline pH this acid dye becomes ionised and hence water-soluble; its release into the aqueous continuous phase can be detected via UV/Vis spectrophotometry at 490 nm.[6] Nanocomposite colloidosomes were prepared using an acidic aqueous phase and sunflower oil containing PPG-TDI

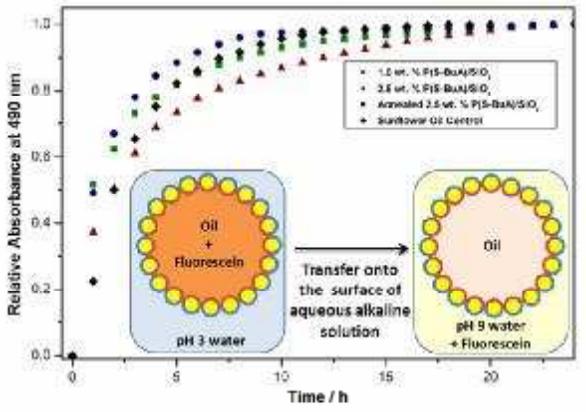

Fig. 11 Release curves obtained at pH 9 for fluorescein dye diffusing from: (■, ▲) covalently cross-linked poly(styrene-co-*n*-butyl acrylate)/silica colloidosomes prepared at different concentrations, (●) annealed colloidosomes and (♦) a sunflower oil control. In all cases the release of fluorescein occurs at essentially the same rate and is complete within 24 h.

cross-linker plus a small quantity of fluorescein (1 mg ml^{-1}). It was evident that the fluorescein was successfully encapsulated inside the oil droplets due to the pink colouration of the (creamed) Pickering emulsions. The droplet size distributions of these colloidosomes were comparable to those prepared without fluorescein and the microcapsules remained stable upon the addition of base. To detect the rate of dye release, a fixed volume of the colloidosomes was pipetted onto the surface of an alkaline aqueous solution (pH 9) in a cuvette. The oil droplets remained on the surface of the aqueous phase due to their low density, and the release of the dye into the basic water was monitored over time.

Figure 11 shows the release curves obtained for the pH-triggered release of fluorescein from various covalently cross-linked nanocomposite colloidosomes and also a pure sunflower oil control. The absorbance due to the fluorescein in the aqueous

phase steadily increased over time as this dye diffuses out of the colloidosomes. Notably, the release rate of the dye from pure sunflower oil occurs over the same time scale as from poly(styrene-*n*-butyl acrylate)/silica colloidosomes, with full release occurring within 24 h. Unsurprisingly, the release rate was insensitive to droplet diameter, which was varied by using a range of nanocomposite particle concentrations. In an attempt to retard the release of the dye, the nanocomposite-stabilised Pickering emulsions were not only cross-linked, but also heated above the T_g of the polymeric core (50 °C) in order to remove any defects present in the microcapsule shell. However, in all cases no detectable retardation of dye release was observed.

The release of fluorescein dye from silica colloidosomes proved to be much more problematic to investigate. Unlike for the poly(styrene-co-*n*-butyl acrylate)/silica nanocomposite particles, the combination of fluorescein dye and PPG-TDI in the oil phase did not allow the formation of silica stabilised emulsions at low pH. The addition of acid and electrolyte did yield stable colloidosomes, but unfortunately on addition to the surface of alkaline solution the microcapsules began to sediment and hence interfere with the UV/Vis measurements.

Conclusions

Glycerol-functionalised colloidal silica sol and core-shell polymer/silica nanocomposite particles can be used to prepare oil-in-water Pickering emulsions at low pH using sunflower oil. Addition of PPG-TDI cross-linker to the oil phase produces covalently cross-linked colloidosomes via urethane chemistry. There is evidence that this cross-linker stabilises these emulsions to the addition of base and colloidosomes remain intact after an alcohol challenge with excess isopropanol. Colloidosomes are not formed in the absence of PPG-TDI. As expected, the mean emulsion droplet diameter decreases with increasing emulsifier concentration. Colloidosomes can be observed by SEM, but they are collapsed under ultra-high vacuum conditions. When poly(styrene-co-*n*-butyl acrylate)/silica nanocomposite particles form the colloidosome shell, individual particles cannot be distinguished by SEM due to their film-forming nature. When investigated by TEM, both silica and polymer are clearly present, although their core-shell nature is difficult to verify. Release of fluorescein into alkaline solution is observed to be almost complete after 24 h in all cases investigated. This indicates that such colloidosomes are inherently permeable and thus cannot retain oil-soluble molecular cargoes.

Acknowledgements

The University of Sheffield is thanked for funding a PhD studentship for LAF.

Notes and references

[a] *Dainton Building, Department of Chemistry, The University of Sheffield, Brook Hill, Sheffield, S3 7HF, UK. Tel: +44-1142-229459; E-mail: l.a.fielding@sheffield.ac.uk*

1. A. D. Dinsmore, M. F. Hsu, M. G. Nikolaides, M. Marquez, A. R. Bausch and D. A. Weitz, *Science*, 2002, **298**, 1006-1009.
2. F. J. Rossier-Miranda, C. Schroen and R. M. Boom, *Colloid Surf. A-Physicochem. Eng. Asp.*, 2009, **343**, 43-49.
3. S. Biggs, R. Williams, O. Cayre and Q. Yuan, 2009, WO/2009/037482.
4. S. Laib and A. F. Routh, *J. Colloid Interface Sci.*, 2008, **317**, 121-129.
5. K. L. Thompson and S. P. Armes, *Chem. Commun.*, 2010, **46**, 5274-5276.
6. K. L. Thompson, S. P. Armes, J. R. Howse, S. Ebbens, I. Ahmad, J. H. Zaidi, D. W. York and J. A. Burdis, *Macromolecules*, 2010, **43**, 10466-10474.
7. A. Walsh, K. L. Thompson, S. P. Armes and D. W. York, *Langmuir*, 2010, **26**, 18039-18048.
8. H. N. Yow and A. F. Routh, *Langmuir*, 2009, **25**, 159-166.
9. S. A. F. Bon, S. Cauvin and P. J. Colver, *Soft Matter*, 2007, **3**, 194-199.
10. O. D. Velev, K. Furusawa and K. Nagayama, *Langmuir*, 1996, **12**, 2385-2391.
11. O. D. Velev, K. Furusawa and K. Nagayama, *Langmuir*, 1996, **12**, 2374-2384.
12. O. D. Velev and K. Nagayama, *Langmuir*, 1997, **13**, 1856-1859.
13. O. J. Cayre, P. F. Noble and V. N. Paunov, *J. Mater. Chem.*, 2004, **14**, 3351-3355.
14. Q. C. Yuan, O. J. Cayre, S. Fujii, S. P. Armes, R. A. Williams and S. Biggs, *Langmuir*, 2010, **26**, 18408-18414.
15. O. J. Cayre and S. Biggs, *J. Mater. Chem.*, 2009, **19**, 2724-2728.
16. H. W. Duan, D. Y. Wang, N. S. Sobal, M. Giersig, D. G. Kurth and H. Mohwald, *Nano Lett.*, 2005, **5**, 949-952.
17. H. L. Wang, X. M. Zhu, L. Tsarkova, A. Pich and M. Moller, *ACS Nano*, 2011, **5**, 3937-3942.
18. S. Simovic and C. A. Prestidge, *Langmuir*, 2008, **24**, 7132-7137.
19. S. A. F. Bon and T. Chen, *Langmuir*, 2007, **23**, 9527-9530.
20. H. Skaff, Y. Lin, R. Tangirala, K. Breitenkamp, A. Böker, T. P. Russell and T. Emrick, *Adv. Mater.*, 2005, **17**, 2082-2086.
21. S. U. Pickering, *Journal of the Chemical Society*, 1907, **91**, 2001-2021.
22. P. F. Noble, O. J. Cayre, R. G. Alargova, O. D. Velev and V. N. Paunov, *J. Am. Chem. Soc.*, 2004, **126**, 8092-8093.
23. L. M. Croll and H. D. H. Stöver, *Langmuir*, 2003, **19**, 10077-10080.
24. R. K. Shah, J. W. Kim and D. A. Weitz, *Langmuir*, 2010, **26**, 1561-1565.
25. S. Levine, B. D. Bowen and S. J. Partridge, *Colloids and Surfaces*, 1989, **38**, 325-343.
26. B. P. Binks and S. O. Lumsdon, *Physical Chemistry Chemical Physics*, 1999, **1**, 3007-3016.
27. S. Fujii, E. S. Read, B. P. Binks and S. P. Armes, *Adv. Mater.*, 2005, **17**, 1014-1018.
28. S. Fujii, S. P. Armes, B. P. Binks and R. Murakami, *Langmuir*, 2006, **22**, 6818-6825.
29. T. N. Hunter, R. J. Pugh, G. V. Franks and G. J. Jameson, *Adv. Colloid Interface Sci.*, 2008, **137**, 57-81.
30. M. Gill, S. P. Armes, D. Fairhurst, S. N. Emmett, G. Idzorek and T. Pigott, *Langmuir*, 1992, **8**, 2178-2182.
31. S. Maeda and S. P. Armes, *J. Mater. Chem.*, 1994, **4**, 935-942.
32. S. Maeda, R. Corradi and S. P. Armes, *Macromolecules*, 1995, **28**, 2905-2911.
33. M. G. Han and S. P. Armes, *J. Colloid Interface Sci.*, 2003, **262**, 418-427.

34. M. G. Han and S. P. Armes, *Langmuir*, 2003, **19**, 4523-4526.
35. M. J. Percy, C. Barthet, J. C. Lobb, M. A. Khan, S. F. Lascelles, M. Vamvakaki and S. P. Armes, *Langmuir*, 2000, **16**, 6913-6920.
36. M. J. Percy, J. I. Amalvy, D. P. Randall, S. P. Armes, S. J. Greaves and J. F. Watts, *Langmuir*, 2004, **20**, 2184-2190.
37. A. Schmid, S. Fujii and S. P. Armes, *Langmuir*, 2006, **22**, 4923-4927.
38. D. Dupin, A. Schmid, J. A. Balmer and S. P. Armes, *Langmuir*, 2007, **23**, 11812-11818.
39. A. Schmid, S. Fujii, S. P. Armes, C. A. P. Leite, F. Galembeck, H. Minami, N. Saito and M. Okubo, *Chem. Mater.*, 2007, **19**, 2435-2445.
40. A. Schmid, J. Tonnar and S. P. Armes, *Adv. Mater.*, 2008, **20**, 3331-3336.
41. L. A. Fielding, J. Tonnar and S. P. Armes, *Langmuir*, 2011, **27**, 11129-11144.
42. A. Schmid, S. P. Armes, C. A. P. Leite and F. Galembeck, *Langmuir*, 2009, **25**, 2486-2494.
43. J. A. Balmer, A. Schmid and S. P. Armes, *J. Mater. Chem.*, 2008, **18**, 5722-5730.
44. H. Zou, S. S. Wu and J. Shen, *Chem. Rev.*, 2008, **108**, 3893-3957.
45. T. Wang and J. L. Keddie, *Adv. Colloid Interface Sci.*, 2009, **147-148**, 319-332.
46. M. J. Burchell, M. J. Willis, S. P. Armes, M. A. Khan, M. J. Percy and C. Perruchot, *Planet. Space Sci.*, 2002, **50**, 1025-1035.
47. R. Srama, W. Woiwode, F. Postberg, S. P. Armes, S. Fujii, D. Dupin, J. Ormond-Prout, Z. Sternovsky, S. Kempf, G. Moragas-Kiostermeyer, A. Mocker and E. Grun, *Rapid Commun. Mass Spectrom.*, 2009, **23**, 3895-3906.
48. Z. Xue and H. Wiese, 2006, United States Patent US7094830B7094832.
49. A. Schmid, P. Scherl, S. P. Armes, C. A. P. Leite and F. Galembeck, *Macromolecules*, 2009, **42**, 3721-3728.
50. P. Greenwood and H. Lagnemo, 2004, WO2004/035474A035471.
51. J. A. Balmer, O. O. Mykhaylyk, A. Schmid, S. P. Armes, J. P. A. Fairclough and A. J. Ryan, *Langmuir*, 2011, **27**, 8075-8089.
52. J. A. Balmer, *PhD Thesis: Colloidal Nanocomposite Particles by Heteroflocculation*, The University of Sheffield, UK, 2010.
53. L. A. Fielding, O. O. Mykhaylyk, S. P. Armes, P. W. Fowler, V. Mittal and S. Fitzpatrick, *Langmuir*, 2012, **28**, 2536-2544.
54. P. Greenwood, *PhD Thesis: Surface Modifications and Applications of Aqueous Silica Sols*, Chalmers University of Technology, Sweden, 2010.
55. D. Lee, J. A. Balmer, A. Schmid, J. Tonnar, S. P. Armes and J. J. Titman, *Langmuir*, 2010, **26**, 15592-15598.
56. I. Blute, R. J. Pugh, J. van de Pas and I. Callaghan, *J. Colloid Interface Sci.*, 2007, **313**, 645-655.
57. Q. C. Yuan, O. J. Cayre, M. Manga, R. A. Williams and S. Biggs, *Soft Matter*, 2010, **6**, 1580-1588.
58. K. L. Thompson, S. P. Armes and D. W. York, *Langmuir*, 2011, **27**, 2357-2363.
59. M. Williams, S. P. Armes and D. W. York, *Langmuir*, 2012, **28**, 1142-1148.